ACS Sustainable Chemistry & Engineering

pubs.acs.org/journal/ascecg

Research Article

Superamphiphobic Surfaces with Self-Cleaning and Antifouling Properties by Functionalized Chitin Nanocrystals

Xianfeng Ou, Jiabing Cai, Jinhuan Tian, Binghong Luo, and Mingxian Liu*

Cite This: *ACS Sustainable Chem. Eng.* 2020, 8, 6690−6699

Read Online

ACCESS | Metrics & More | Article Recommendations | Supporting Information

ABSTRACT: Superamphiphobic coating has significant applications in self-cleaning and antifouling materials. Herein, chitin nanocrystals (ChNCs) with a needlelike morphology as building blocks were modified by thiol groups and highly fluorinated long chains to reduce the surface free energy. For the prepared superamphiphobic ChNC particles, a series of morphological and physicochemical characterizations, such as transmission electron microscopy, scanning electron microscopy, Fourier transform infrared spectroscopy, X-ray diffraction, thermogravimetric analysis, and X-ray photoelectron spectroscopy, were performed. The superamphiphobic ChNC particles feature high contact angles and low sliding angles for various liquids, including *n*-decane with a low surface tension (23.3 mN/m). Different liquid droplets can retain a perfectly quasispherical shape on the coating surface. Most interestingly, liquid marbles wrapped up by this superamphiphobic powder can "stand" on various substrates without any collapse. The coating shows a good repellency for liquids after the mechanical damage tests and thermal treatments. In addition, the superamphiphobic ChNC particles could be applied onto various substrates, exhibiting a good resistance and substrate-independent performance. In sum, the fluorinated ChNC coatings with superior superamphiphobicity, substrate independence, and stable mechanical and thermal properties show promising applications of water/oil-proof, self-cleaning, and antifouling coatings.

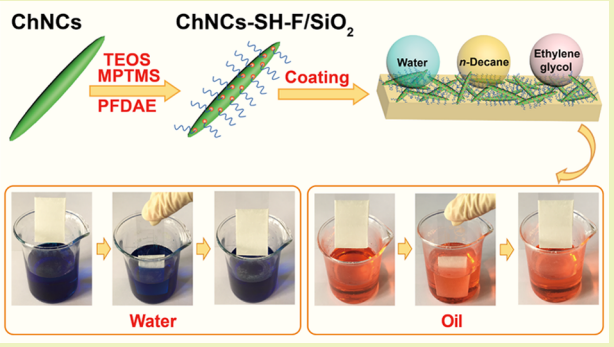

KEYWORDS: *chitin nanocrystals, fluorinated, coating, superamphiphobic, self-cleaning*

INTRODUCTION

Biomimetic superamphiphobic surfaces have aroused great research interest in recent decades, inspired by the self-cleaning phenomenon in nature.[1−3] Lotus leaf has an outstanding self-cleanable property even though it grows in mud, attributed to the presence of micro-/nanostructured mastoids and waxes on its surface.[4,5] Learning from the lotus leaf effect, numerous artificial superhydrophobic/superamphiphobic surfaces have been fabricated considering their broad perspective in self-cleaning,[6] corrosion resistance,[7] anti-icing/antifogging,[8,9] antibacterial surface,[10] and water/oil separation.[11,12] Generally, a superamphiphobic surface is requested with a high contact angle (>150°) and small roll-off angle (<10°), which can repel various liquids with different surface tensions.

A large number of approaches to construct such artificial superamphiphobic surfaces have been reported, such as laser and chemical etching, phase separation, electrochemical deposition, electrospinning, and the sol−gel method. For example, the hierarchical superhydrophobic surfaces with well-ordered secondary nanostructures were fabricated using an electron-beam lithography technique and further modified with a fluoroalkylsilane via a vapor-phase reaction.[13] A superhydrophobic porous film with a contact angle of 155.1° and a sliding angle of 6.5° was fabricated by a phase separation method, and meanwhile its surface energy was reduced via the modification of fluorinated acrylic polymer resin.[14] A dual-scale structured superamphiphobic surface with nano-Ni pyramid/micro-Cu cone structures was prepared by an electrochemical deposition process and facial modification with per-fluorinated chains, exhibiting excellent repellence for water and ethylene glycol.[15] A robust superamphiphobic coating film was obtained via electrospinning rice-shaped TiO_2 nanostructures coupled with fluorinated silanes, achieving a high contact angle of water (166 ± 0.9°) and hexadecane (138.5 ± 1°).[16] To sum up, this synergistic effect of macro-/nanostructured geometry and ultralow surface energy is crucial to create a superamphiphobic surface via diverse methods of surface modification.

Numerous nanostructured materials from nature are employed for the manufacture of superamphiphobic coatings via surface modification using ultralow-surface-energy chemicals (fluorinated compounds in general). Due to their nanoscale,

Received: January 14, 2020
Revised: April 1, 2020
Published: April 8, 2020

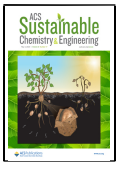

https://dx.doi.org/10.1021/acssuschemeng.0c00340
ACS Sustainable Chem. Eng. 2020, 8, 6690−6699

abundant surface groups, high-specific-area surfaces, and ease of preparation, many nanoparticles have been exploited in the fields of self-cleaning and antifouling, including carbon nanotubes, natural palygorskite nanorods, and halloysite nanotubes. For instance, carbon nanotubes were used to construct a hierarchical lotus-leaf-like structure in a coating prior to the fluorinated modification, which showed an excellent nonwetting property under a harsh environment.[17] Natural palygorskite nanorods acted as the building blocks for superamphiphobic coatings via grafting of organosilanes, exhibiting low sliding angles and high mechanical, environmental, chemical, and thermal durability.[18] Due to their unique hollow nanotubular nanostructure and abundant surface groups, halloysite nanotubes were functionalized with biomimetic catechol-bearing fluoropolymers and the coatings showed antiwetting characteristics to various liquids with a broad range of surface tensions.[19]

Chitin nanocrystals (ChNCs), with a unique needlelike nanostructure, are obtained from a naturally available polysaccharide of chitin.[20] The advantages of ChNCs include high aspect ratios, high specific surface area, plenty of surface functional groups, and biodegradability.[21,22] ChNCs exhibit lengths and widths of 100−500 and 15−30 nm, respectively, possessing an aspect ratio of 3−16.[23,24] One-dimensional ChNCs have an elongated structure, which is of great benefit for high surface roughness. It was reported that the wettability of MoS_2 can be controlled by multiscale modulation of surface roughness by tuning of nanoflower structures using chemical vapor deposition and microscale topography via mechanical strain.[25] In another report, a monolithic platform based on three-dimensional (3D) multiscale hierarchical wrinkles of poly(dimethysiloxane) was developed, which can be functionalized as static and dynamical water-repellent substrates.[26] Therefore, tailoring the surface roughness of nanomaterials by various processing methods is an effective way to adjust the surface wetting properties. The stacked ChNCs with nanoscale hierarchical structures create lots of micropores, which can trap a layer air bubble around them. Meanwhile, the needlelike morphology of ChNCs could form protrusion structures that increase the surface roughness of a substrate.[27] In addition, abundant surface hydroxyl groups on the surface of ChNCs are prone to grafting with organosilanes (containing chlorosilane or alkoxysilane moieties) with low surface tension, realizing the superamphiphobic modification.[28] For example, SiO_2 particles are prone to depositing on ChNCs by hydrolysis of tetraethyl orthosilicate (TEOS). Therefore, ChNCs are promising nanomaterials for the construction of a hierarchical macro-/nanostructured surface and modification with ultralow-surface-energy chemicals, which can exhibit excellent antiwettability for water and organic solvents. Compared with other nanoparticles, ChNCs are a kind of novel renewable polysaccharide nanomaterials that show a great promise as a functional material for nanofillers in polymer composites, drug delivery carriers for controlling release, electronic materials for energy saving, optical materials for field-emission devices, and degradable materials for an eco-friendly package. Therefore, tailoring the wettability of ChNCs by surface functionalization and construction of the hierarchical microstructure is significant for these critical applications. However, ChNCs acting as building blocks in the application of superamphiphobic coating have not yet been reported.

In this work, a green and sustainable polysaccharide nanomaterial of ChNCs is used to prepare superamphiphobic coating. ChNCs as the fundamental building blocks can create a hierarchical macro-/nanostructured surface coating with low surface tension. Thiol-group functionalized ChNC particles were synthesized via a sequence of hydrolysis and co-condensation reactions of TEOS and (3-mercaptopropyl) trimethoxysilane, to create a quasi-lotus-leaf structure with a superhydrophobic property. Thiol-group functionalized ChNC particles were then modified into a superamphiphobic structure by combining with fluorinated long chains. As-prepared superamphiphobic particles were coated on various substrates through simple yet versatile methods (deposition with double-sided tape, spray-coating, dip-coating, and filtering). The superamphiphobic coatings exhibit excellent water and oil repellency and high mechanical and thermal stability, showing promise in fields like self-cleaning and antifouling.

EXPERIMENTAL SECTION

Chemicals and Materials. Chitin was purchased from Wuhan Hezhong Biochemical Manufacturing Co., Ltd., China. Hydrochloric acid (HCl, 37%) was obtained from Guangzhou chemical reagent factory. Tetraethyl orthosilicate (TEOS, 98%) was supplied by Tianjin Baishi Chemical Co., Ltd., China. (3-Mercaptopropyl) trimethoxysilane (MPTMS, 95%) was purchased from Shanghai Aladdin Co., Ltd., China. 1*H*,1*H*,2*H*,2*H*-Heptadecafluorodecyl acrylate (PFDAE, 98%) was provided by Shanghai Energy Chemical Co., Ltd., China. Benzoin dimethyl ether (DMPA, 99%) was supplied by Shanghai Macklin Biochemical Co., Ltd., China. Water was purified by a Milli-Q water system (resistivity > 18.2 MΩ/cm).

Preparation of Chitin Nanocrystals (ChNCs). Twenty grams of chitin and HCl (600 mL, 3 mol/L) were heated in an oil bath at 104 °C for 5 h. Then, the mixture was washed using ultrapure water at least three times by centrifugation. After that, the mixture was dialyzed in flowing water for 24 h to further remove the remaining HCl. The suspension was dried by a SCIENTZ-12ND vacuum freeze dryer (Ningbo Scientz Biotechnology Co., Ltd., China), and ChNC powder was finally obtained.

Preparation of Superhydrophobic Thiol-Group Functionalized ChNCs/SiO_2 (ChNCs-SH/SiO_2) Powder. First, 5 g of ChNCs was ultrasonically dispersed into the mixtures (260 mL) of absolute ethanol and ammonia hydroxide (v/v = 25:1) for 0.5 h. Then, 12 mL of TEOS was added into the above mixtures drop by drop under vigorous stirring. Twelve milliliters of MPTMS was then added and stirred continuously at room temperature for 24 h. After that, the reactant mixture was heated at 80 °C under magnetic stirring for 2 h. The solid product was washed with absolute ethanol at least three times by centrifugation. ChNCs-SH/SiO_2 powder was finally collected and dried at 60 °C.

Preparation of Superamphiphobic Fluorinated Functionalized ChNCs-SH/SiO_2 (ChNCs-SH-F/SiO_2) Powder. To obtain ChNCs-SH-F/SiO_2, 2.5 g of the prepared ChNCs-SH/SiO_2 was ultrasound-dispersed with a mixture of absolute ethanol (250 mL) and PFDAE (2.5 g) for 0.5 h. ChNCs-SH/SiO_2 particles were fluorine-functionalized by the treatment of UV light (365 nm, 99 mW/cm^2) with the initiator of 0.5 wt % DMPA for 20 min. The solid product was washed with absolute ethanol at least three times by centrifugation. ChNCs-SH-F/SiO_2 powder was finally collected and dried at 60 °C. The synthesis process of superamphiphobic ChNCs-SH-F/SiO_2 particles is schematically illustrated in Figure 1. First, TEOS was hydrolyzed into orthosilicic acid in ammonia solution and then interacted with −OH groups on the ChNC surface. Subsequently, MPTMS was hydrolyzed into silicic acid with thiol groups, which was then condensed with ChNCs/SiO_2 to obtain ChNCs-SH/SiO_2.[29,30] ChNCs-SH/SiO_2 was then chemically reacted with PFDAE using a UV-initiated thiol-ene click reaction, and the prepared ChNCs-SH-F/SiO_2 particles exhibited superamphiphobicity.[31]

Preparation of ChNCs-SH-F/SiO_2 Coatings on Various Materials. The superamphiphobic ChNCs-SH-F/SiO_2 powder was coated on various substrates (glass slide, polyethylene plastic, polyurethane sponge, cotton, and filter paper) with various methods

https://dx.doi.org/10.1021/acssuschemeng.0c00340
ACS Sustainable Chem. Eng. 2020, 8, 6690−6699

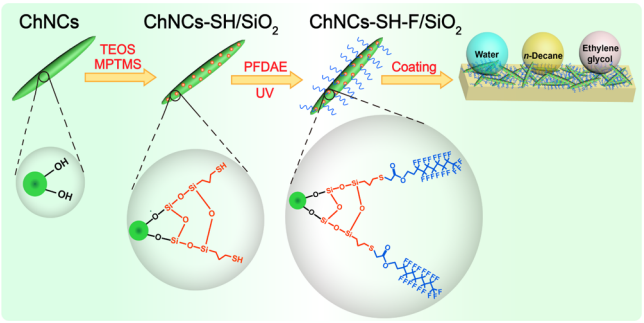

Figure 1. Schematic illustration of the preparation process of ChNCs-SH-F/SiO_2.

(deposition with double-sided tape, spray-coating, dip-coating, and filtering), as illustrated in Figure 2. A glass slide was pasted on a thin

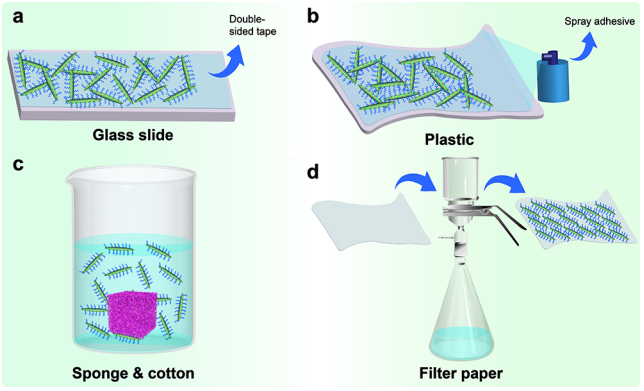

Figure 2. ChNCs-SH-F/SiO_2 powder coated on different substrates with various methods (deposition with double-sided tape (a), spray-coating (b), dip-coating (c), and filtering (d)).

layer of double-sided tape (Deli, China) (Figure 2a), while the surface of the plastic membrane was covered with spray adhesive (Super 77, 3 M) (Figure 2b). The pretreated surface of the glass slide and plastic membrane was sprinkled with a layer of superamphiphobic powder. Sponge and cotton with pore structures were coated on superamphiphobic particles by stirred-dipping in the 6 wt % ChNCs-SH-F/SiO_2/ethanol suspension for 24 h (Figure 2c). Coated sponge and cotton were obtained after drying at 60 °C. Coated filter paper was obtained by vacuum filtration of the ChNCs-SH-F/SiO_2/ethanol suspension (Figure 2d).

Characterization. The morphology of ChNCs, ChNCs-SH/SiO_2, and ChNCs-SH-F/SiO_2 was examined using transmission electron microscopy (TEM) (JEM-2100F, JEOL Ltd., Japan). The surface morphology of samples after spraying a thin gold layer was analyzed by scanning electron microscopy (SEM) (Ultra 55 SEM instrument, ZEISS, Germany) with a voltage of 5 kV. The Fourier transform infrared spectroscopy (FTIR) instrument (Nicolet iS50, Thermo Fisher Scientific Ltd., USA) was used to analyze the FTIR spectra of ChNCs, ChNCs-SH/SiO_2, and ChNCs-SH-F/SiO_2 from 4000 to 500 cm^{-1}. The crystal structure of the samples was characterized on an X-ray diffractometer (XRD) (MiniFlex-600, Rigaku Corp., Japan) from 3 to 50°. The thermoanalysis of the samples was conducted by a thermogravimetric (TGA) instrument (Mettler Toledo, Switzerland) with an increased speed of 10 °C/min ranging from 50 to 600 °C under a N_2 atmosphere. The surface chemical component analysis of ChNCs, ChNCs-SH/SiO_2, and ChNCs-SH-F/SiO_2 was carried out with an X-ray photoelectron spectroscopy (XPS) instrument (K-Alpha$^+$, Thermo Fisher Scientific Co., Ltd., USA). The surface morphology and roughness of the glass substrate coating were analyzed with a 3D optical profilometer (UP-DUAL MODE, Rtec Engineering Ltd., USA) with a scanning area of 1 mm × 1 mm. The water and oil repellency of the samples was measured on a contact angle instrument (DSA100, Kruss Ltd., Germany) at room temperature. The volume of tested liquids for contact angles and roll-off angles was 5 and 10 μL, respectively. Each data was reliably obtained by testing the sample five times.

Thermal Stability Evaluation. The ChNCs-SH-F/SiO_2 powder was treated at −74, −5, 100, 150, and 200 °C, respectively. To evaluate thermal stability, the water/oil contact angles of the pretreated powder were measured. At least five measurements were reliably recorded for each sample.

Mechanical Stability Tests. For the abrasion stability test, the coated glass slide was abraded with a piece of sandpaper (2000 Cw) under the weight of 100 g as a typical representative. This coated glass slide was abraded 10 times with a distance of 10 cm. Meanwhile, the performance of mechanical durability was further investigated via treatments with tissue wipe, tape peeling, and blade scratching.[32] Then, the mechanical durability of coated substrates was evaluated through contact angles and roll-off angles after the mechanical damages.

RESULTS AND DISCUSSION

Characterizations of Superamphiphobic ChNCs-SH-F/SiO_2 Powder. Microstructures of ChNCs, ChNCs-SH/SiO_2, and ChNCs-SH-F/SiO_2 were observed by TEM and SEM, as shown in Figure 3a,b. ChNCs show a homogeneously nanoneedlelike structure with length and width ranges of 100−500 and 15−30 nm, respectively. So the aspect ratio of ChNCs is 3−16. It should be noticed that the size of ChNCs is dependent on the resources of chitin and the reaction time.[22] ChNCs-SH/SiO_2 and ChNCs-SH-F/SiO_2 exhibit rougher surfaces and poorer dispersivity compared with unmodified ChNCs, illustrating that an amphiphobic thiol group and a fluorinated long chain were grafted onto the ChNC surface. Meanwhile, the SiO_2 particles were deposited on the surface of ChNCs during the synthesis of thiol-group functionalized ChNCs. ChNCs-SH/SiO_2 and ChNCs-SH-F/SiO_2 have low surface coverage in both TEM and SEM images compared with raw ChNCs, which is caused by particle aggregation after modification. Needlelike ChNCs with a high aspect ratio are favorable to creating nanoscale protrusions on the coating surface.

ChNCs-SH/SiO_2 and ChNCs-SH-F/SiO_2 were also studied by FTIR spectra (Figure 3c). In the spectrum of raw ChNCs, the peaks at 3260, 1647, and 1560 cm^{-1} are assigned to the N−H stretching vibration, amide I, and amide II, suggesting a typical α-chitin structure.[33] Compared with raw ChNCs, new bands of the modified ChNCs appear at 2930, 2567, and 805 cm^{-1} attributed to the $-CH_2$ stretching vibrations, S−H stretching vibrations, and Si−O−Si symmetric stretching, respectively.[27,34] The appearance of hydrophobic S−H and Si−O−Si groups in the modified ChNC spectrum indicates the successful synthesis of ChNCs-SH/SiO_2 via a series of hydrolysis and co-condensation reactions. The characteristic absorption peaks of the C−F group are identified at 1239 and 1207 cm^{-1},[35] suggesting the copolymerization of amphiphobic fluorinated long chains with ChNCs-SH/SiO_2.

XRD patterns of ChNCs before and after modification are shown in Figure 3d. The typical diffraction peaks of ChNCs appear at 9.3° (020 plane), 19.1° (110 plane), and 26.2° (013 plane).[36] It can be found that the crystalline structure of modified ChNCs does not change. However, the patterns of modified ChNCs emerge as a wide peak centered at 6°, possibly originating from the deposition of SiO_2 on the surface of ChNCs. The thermal degradation behavior of ChNCs, ChNCs-SH/SiO_2, and ChNCs-SH-F/SiO_2 is shown in Figure 3e,f. The weight of ChNCs begins to decrease because of the loss of

https://dx.doi.org/10.1021/acssuschemeng.0c00340
ACS Sustainable Chem. Eng. 2020, 8, 6690−6699

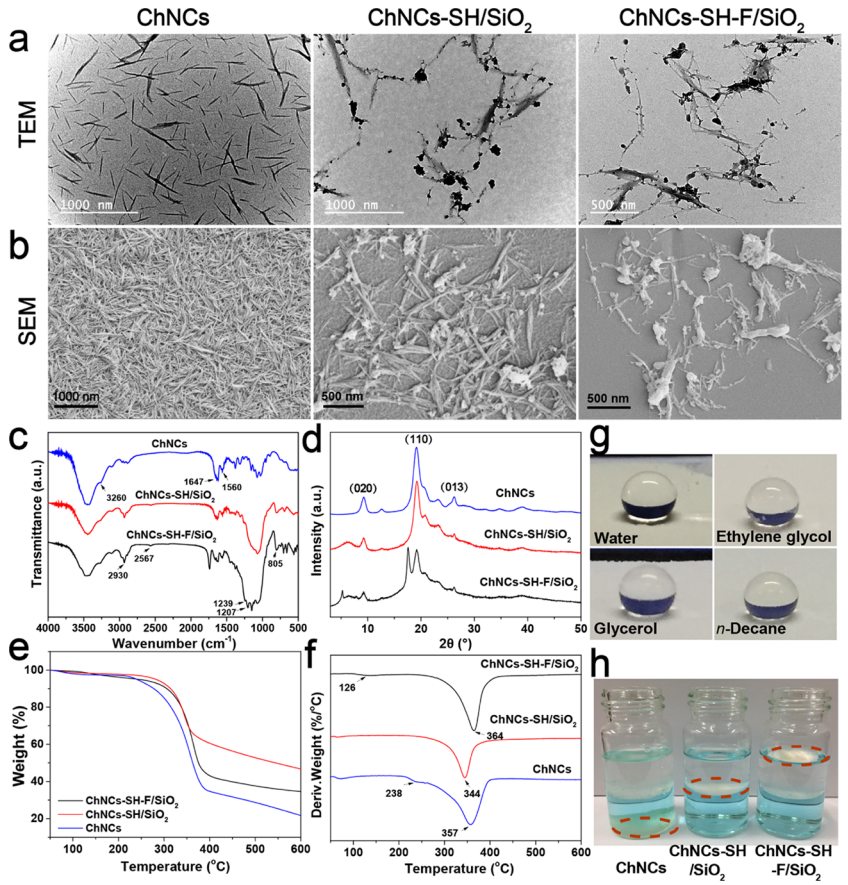

Figure 3. TEM photographs (a), SEM photographs (b), FTIR spectra (c), XRD patterns (d), TG (e), and derivative thermogravimetry (DTG) (f) of ChNCs, ChNCs-SH/SiO_2, and ChNCs-SH-F/SiO_2 particles; images of droplets (water, ethylene glycol, glycerol, and *n*-decane) on ChNCs-SH-F/SiO_2 powder (g); images of the dispersion state for the powders in the oil/water (dyed blue) mixtures (h).

adsorbed water under 100 °C, indicating the hydrophilicity of ChNCs. The initial degradation temperatures of ChNCs, ChNCs-SH/SiO_2, and ChNCs-SH-F/SiO_2 are 224, 257, and 276 °C, respectively, and the maximum decomposition temperatures of the samples are 357, 344, and 364 °C, respectively. The increased initial degradation temperatures of modified ChNCs may be attributed to the graft of SiO_2, S−H, and fluorinated long chain. ChNCs-SH-F/SiO_2 almost completely decomposes at the highest temperature of about 434 °C in comparison with ChNCs (405 °C) and ChNCs-SH/SiO_2 (412 °C). This suggests a high thermal stability of ChNCs-SH-F/SiO_2, implying that this particle still maintains its physicochemical performance below 200 °C, which is consistent with the following thermal stability test of the prepared superamphiphobic coating.

As shown in Figure 3g, various droplets (water, ethylene glycol, glycerol, and *n*-decane) exhibit a stable spherical shape on the surface of the mechanical-pressed ChNCs-SH-F/SiO_2 powder without any penetration. Therefore, ChNCs-SH-F/SiO_2 powder by the fluorinated modification exhibits strong repulsive interaction for water and organic solvents with different surface tensions. The dispersion of ChNCs-SH-F/SiO_2 powder in the oil/water (dyed blue) mixtures was compared to that of ChNCs and ChNCs-SH/SiO_2 (Figure 3h). Unmodified ChNCs are dispersed in water. However, ChNCs-SH/SiO_2 floats in the medium interface between oil and water whileChNCs-SH-F/SiO_2 floats on top of the oil surface, further suggesting that ChNCs-SH/SiO_2 powder without the fluorinated functionalized modification is hydrophobic but oleophilic, while ChNCs-SH-F/SiO_2 powder is not only hydrophobic but also oleophobic.

To identify the surface chemical components, XPS spectra of ChNCs, ChNCs-SH/SiO_2, and ChNCs-SH-F/SiO_2 were examined (Figure 4). From the spectrum of ChNCs (Figure 4a), the characteristic peaks appear at 535.4, 401.1, and 287.1 eV, assigned to O 1s, N 1s, and C 1s, respectively. In the spectrum of ChNCs-SH/SiO_2 (Figure 4c), the new peaks at 163.6 eV (S 2p) and 105.9 eV (Si 2p) are observed for the reactions of ChNCs with TEOS and MPTMS. A strong peak of F 1s appears at 689.6 eV in the spectrum of ChNCs-SH-F/SiO_2, demonstrating the introduction of high F content (Figure 4e). But the peak of N 1s is not detected in the spectra of ChNCs-SH/SiO_2 and ChNCs-SH-F/SiO_2. It is caused by the fact of XPS scanning on the sample surface, which is covered by the bonding chains. The C 1s core-level spectrum of ChNCs can be deconvoluted to three peak components at 287.9 eV (O−C−O/C═O), 286.6 eV (C−N/C−O), and 284.9 eV (C−C/C−H) (Figure 4b).[37] From the C 1s core-level spectrum of ChNCs-SH/SiO_2 in Figure 4d, the peaks at 286.2, 285.1, and 284.0 eV are ascribed to C−S, C−C/C−H, and C−Si bands, respectively.[38] In addition, as shown in Figure 4f, the C 1s spectrum of ChNCs-SH-F/SiO_2 is deconvoluted to seven peaks at 293.9 eV (CF_3), 291.6 eV ($-CF_2$), 289.0 eV (O−C═O), 287.2 eV (C−O/CH_2−CF_2), 285.7 eV (C−S), 285.0 eV (C−C/C−H), and 283.5 eV (C−Si).[39−41] These new peaks indicate that ChNCs are successfully grafted with thiol groups and

https://dx.doi.org/10.1021/acssuschemeng.0c00340
ACS Sustainable Chem. Eng. 2020, 8, 6690−6699

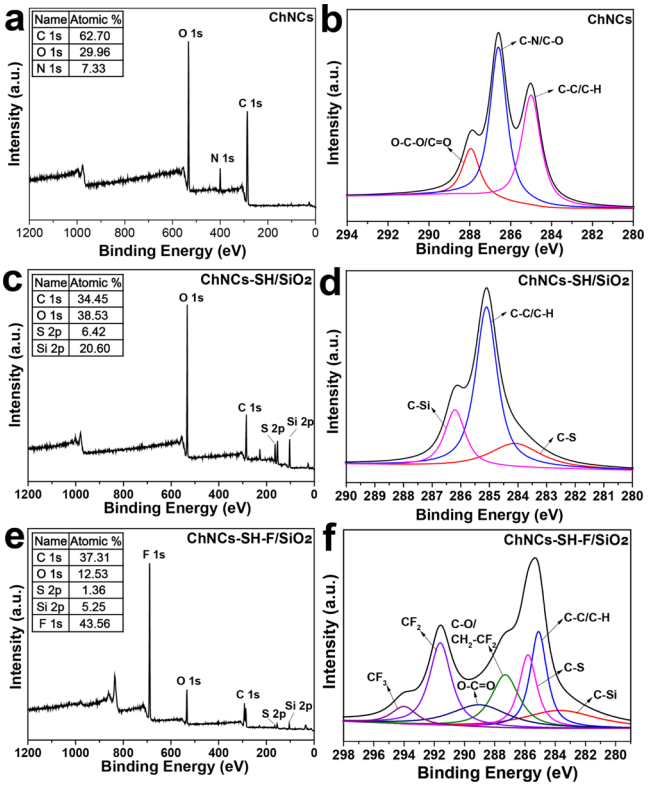

Figure 4. XPS survey spectra and C 1s spectra for ChNCs (a, b), ChNCs-SH/SiO_2 (c, d), and ChNCs-SH-F/SiO_2 (e, f).

fluorinated chain molecules. The C, O, and N atomic ratios of the ChNC surface are 62.70, 29.96, and 7.33%, respectively, while ratios of C, O, S, and Si for ChNCs-SH/SiO_2 are 34.45, 38.52, 6.42, and 20.60%, respectively. In contrast, the C, O, S, Si, and F contents of ChNCs-SH-F/SiO_2 are 37.31, 12.53, 1.36, 5.25, and 43.56%, respectively. A high F content of ChNCs-SH-F/SiO_2 could be attributed to a high grafting ratio of fluorinated chains, which is significant to decrease its surface energy. However, environmental concerns of the decomposition product of the grafted fluoropolymers over a C-8 fluorinated chain were raised. PFDAE with a C-10 fluorinated chain might decompose into perfluorooctanoic acid or perfluorooctanoic sulfonate, which could cause environmental risk because of bioaccumulation and might be carcinogenic.[42] But, the length of the fluorinated chain decides the surface tension of the fluoropolymer. So PFDAE with a C-10 fluorinated chain possesses superior superhydrophobicity in spite of its potential toxicity.

Antiwettability of the Superamphiphobic Coating. To evaluate the nonwettability of ChNCs-SH-F/SiO_2, various liquid droplets with different surface tensions were measured on the superamphiphobic powder. As shown in Figure 5, the contact angles and roll-off angles of water and organic solvents (including glycerol, ethylene glycol, *n*-hexadecane, *n*-decane, sunflower seed oil, and vacuum pump oil) range from 156.2 to 168.1 and 2.9 to 9.3°, respectively, exhibiting strong repellence against water and oils. Especially, the coating features the optimum repelled performance with respect to water for its high surface tension (72.4 mN/m).[43] Interestingly, the coating also can resist against vacuum pump oil with a high viscosity and *n*-decane with a low surface tension (23.3 mN/m).[27,44] *n*-Heptane (surface tension 20.1 mN/m) and *n*-octane (surface tension 21.6 mN/m) droplets were also measured on the ChNCs-SH-F/

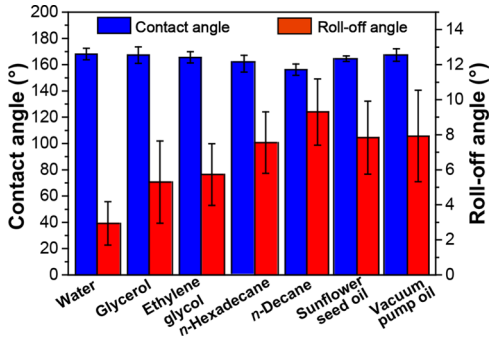

Figure 5. Contact angles and roll-off angles of various liquids on the ChNCs-SH-F/SiO_2 powder.

SiO_2 surface, but both of them exhibit a low contact angle and gradually permeate the surface. It may be hard for the ChNCs-SH-F/SiO_2 surfaces to repel oils with much lower surface tensions. These results indicate that the ChNCs-SH-F/SiO_2 coating displays superior superhydrophobic and superoleophobic properties.

To measure the antiwettability, the water/oil droplet movement tests (including the vertical and horizontal directions) were performed (Figure 6, and Videos S1 andS2).

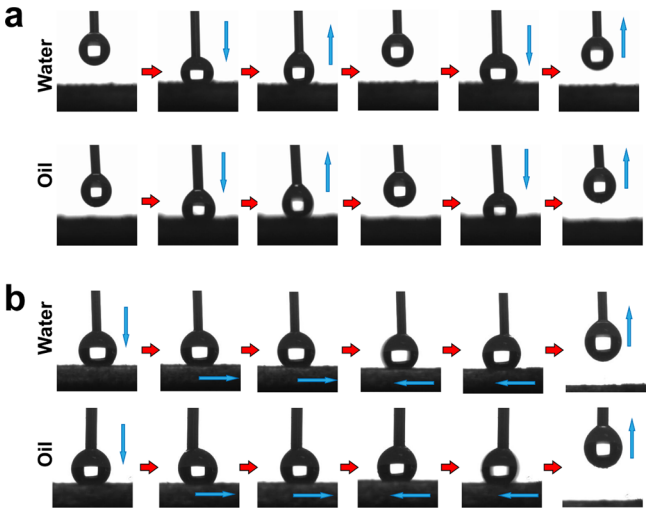

Figure 6. Dynamic interaction between a water/oil droplet and the coating surface (a); antiwettability tests of the coating via back and forth movements (b).

As displayed in Figure 6a, a spherical water droplet hung up in a syringe drops down contacting the superamphiphobic particle-coated glass slide and then goes up leaving the coating surface. After repeating this experiment three times, the water droplet still hangs on the syringe with its original shape without adhesion of any powder and losing of the water. Additionally, a similar result for ethylene glycol is obtained after conducting the interaction experiment two times, while the oil droplet adheres to a little powder on the bottom. As shown in Figure 6b, Videos S1 andS2, once the water/oil droplets encounter the coating substrate, the substrate is parallelly moved back and forth at a constant rate. It can be observed that the droplet remains ball-shaped, which indicates that the surface has low adhesion to water and oil. This result implies that the prepared coating exhibits antiwettability for both water and oil droplets, indicating its super-repellent capacity.

https://dx.doi.org/10.1021/acssuschemeng.0c00340
ACS Sustainable Chem. Eng. 2020, 8, 6690−6699

As shown in Figure 7a, a drop of water (dyed with methylene blue) (~10 μL) is wrapped by a thin layer of ChNCs-SH-F/SiO_2

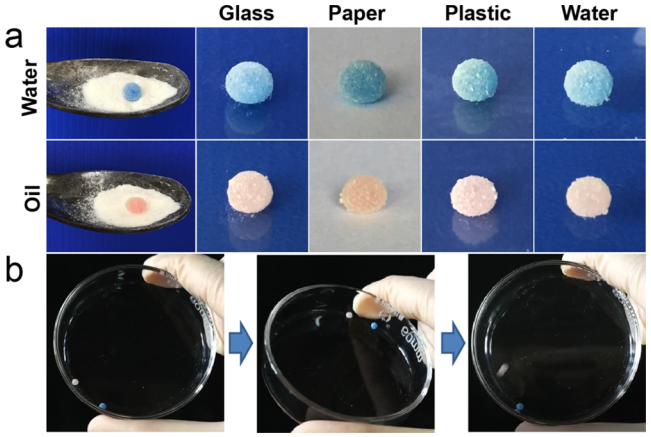

Figure 7. Images (a) of water and oil liquid marbles wrapped up with ChNCs-SH-F/SiO_2 powder on the surfaces of glass, paper, plastic, and water; photographs (b) of the rolling process of the liquid marbles in the glass dish.

powder, when it rolls down to the superamphiphobic powder. The formation process of the red oil marble (dyed with Sudan III) can also be realized. In comparison, the oil marble is much like an oval ball due to the high viscosity, whereas the water marble resembles a quasispherical shape. Furthermore, the prepared liquid marbles can "stand" on various substrates without any infiltration, such as glass, paper, and plastic and even float on water surface. More interestingly, as shown in Figure 7b and Video S3, the liquid marbles perfectly like a little ball can roll around the glass dish and plastic membrane, due to the surface nanoroughness and the low surface free energy of the fluorinated chains outside the ChNCs.[45] In contrast, the rolling motion of the water marble displays more flexibility than the oil marble because of lower viscosity.

Morphology of the Glass Substrate-Coated Superamphiphobic Powder. The 3D surface morphology and roughness of blank and superamphiphobic powder coated on the glass substrates were analyzed by a 3D optical profilometer (Figure 8). It can be observed that the surface of blank glass is smooth with a slight height difference of 3.2 μm in Figure 8a. However, many peaks and valleys appear on the surface of superamphiphobic powder-coated glass substrates so the height difference remarkably increases to 118 μm (Figure 8b). The surface roughness can be quantitatively analyzed by height profile curves. Figure 8c displays a uniform rise-declining curve, showing a flat surface of the uncoated glass substrate. The height profile curve of the coated glass substrate becomes much disordered than that of the blank glass, due to the overlapping of superamphiphobic nanoparticles (Figure 8d). Higher surface roughness of the coating is assigned to the synergistic combination of ChNCs, SiO_2, and the fluorinated chain, which ensures its superamphiphobicity.

Self-Cleaning Function of the Coating. Self-cleaning is a crucial feature of the superamphiphobic ChNCs-SH-F/SiO_2 surface. To study the self-cleanable performance, glass slides with a flat surface were chosen as substrates. As the result shows in Figure 8, the superamphiphobic coating on the glass substrate displays a rough surface, suggesting an antiadhesive surface.[46] As shown in Figure 9a,b, the surface wettability of the ChNCs-SH-F/SiO_2 coating was compared to that of the ChNCs-SH/SiO_2 coating. The ChNCs-SH-F/SiO_2 coating can hold on various aqueous droplets (water, tea, milk, and cola) in a spherelike shape even against corrosive liquids (HCl (3 mol/L) and NaOH (3 mol/L)), whereas *n*-hexadecane spreads out on the ChNCs-SH/SiO_2 coating. This demonstrates that the ChNCs-SH/SiO_2 coating is superhydrophobic but oleophilic, due to the oleophilicity of the grafted silanes.[47] Si−O−Si backbones surrounded by ChNC surfaces provide the reaction sites for the grafting of the hydrophobic $-CH_2-$ groups, which can achieve superhydrophobicity. However, $-CH_2-$ groups without a fluorinated compound cannot resist a majority of organic solvents with much lower surface tensions (e.g., *n*-hexadecane

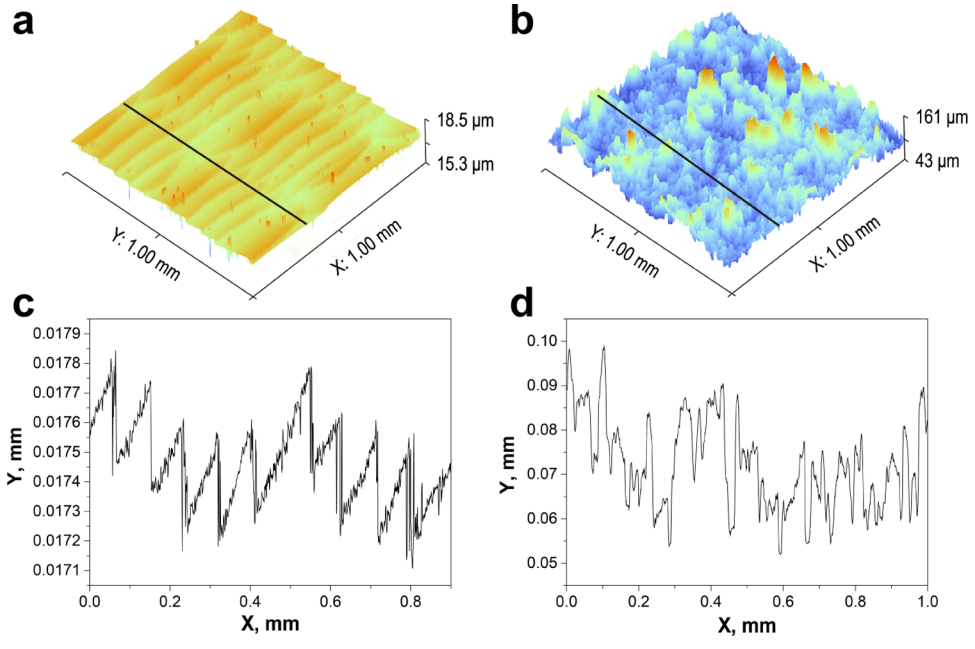

Figure 8. Three-dimensional topography and surface roughness curves of the blank glass (a, c) and ChNCs-SH-F/SiO_2-coated glass (b, d).

https://dx.doi.org/10.1021/acssuschemeng.0c00340
ACS Sustainable Chem. Eng. 2020, 8, 6690−6699

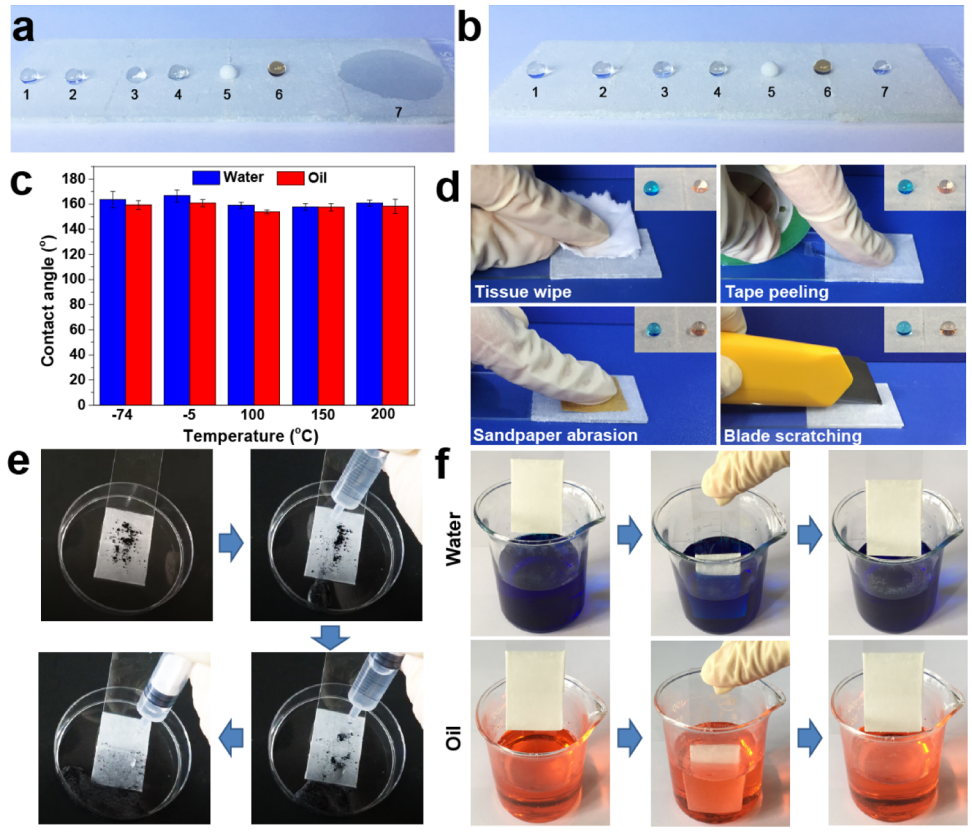

Figure 9. Photographs of various droplets (1: water, 2: HCl, 3: NaOH, 4: tea, 5: milk, 6: cola, and 7: *n*-hexadecane) on glass slides coated with ChNCs-SH/SiO_2 (a) and ChNCs-SH-F/SiO_2 (b); the contact angles (c) of ChNCs-SH-F/SiO_2 particles after treatment at different temperatures; the pictures show the mechanical stability of the coated glass slides with different physical damages (d); self-cleaning and antifouling property of the coated glass slides by carbon black dust (e) and images of coated glass slides immersed in the dyed−water mixtures and oil solution (f).

(27.5 mN/m)). So the fluoropolymer with a $-CF_3$ end group and seven $-CF_2-$ units (surface tension ~7 mN/m) is necessary on the hydrophobic ChNCs-SH/SiO_2 surface.[48] The low surface tension of ChNCs-SH-F/SiO_2 is also caused by large steric repulsion of the fluorinated long chain. Therefore, various aqueous droplets and *n*-hexadecane are both in the Cassie−Baxter state and readily roll off from the ChNCs-SH-F/SiO_2 coating.[49] Considering that the coating may be exposed to different temperatures in real applications, temperature stability tests were performed for the ChNCs-SH-F/SiO_2 coating (Figure 9c). After the treatments in a temperature range of −74−200 °C, the water and oil contact angles of the ChNCs-SH-F/SiO_2 coating are still above 150°, indicating that the main ingredient of particles does not decompose and shows excellent stability at different temperature conditions. Other environmental and chemical durabilities of the prepared superamphiphobic surface, such as under wind and sunlight, will be evaluated in the following work. The mechanical stability of the ChNCs-SH-F/SiO_2 coating is also assessed (Figure 9d). As shown in the insets, the coatings can hold on a stable water/oil droplet after damage treatments with tissue wipe, tape peeling, sandpaper abrasion, and blade scratching. To evaluate the mechanical strength, a coated glass sheet was abraded with a piece of sandpaper under a load of 100 g (see Video S4). Although a little powder falls down on the coated glass slide, the abraded surface still readily rolls off the water and oil droplets even after abrading 10 times. This result suggests that ChNCs-SH-F/SiO_2 particles can be firmly adherent by the method of double-sided tape and the coating surface retains a hierarchical micro/nano dual-scale structure, even though it suffers from mechanical wear. Moreover, SEM results reported in previous studies suggested that the composition and structure of the superamphiphobic surface did not change after the abrasion with sandpaper.[50−52] So the ChNCs-SH-F/SiO_2-coated surface could resist slight mechanical damages and remain superamphiphobic. The antifouling property of the ChNCs-SH-F/SiO_2 coating was further investigated. Small carbon black particles as the contamination deposited on the coating surface could be rolled off along with water droplets, suggesting weak interaction between liquid droplets and the coating (Figure 9e and Video S5). After the water washing, the coated surface finally becomes clear even if it is contaminated by the strong-stained carbon black particles. Concerning dye-/oil-fouling resistance, the coated glass was separately immersed in the methylene blue solution and cooking oil (Figure 9f and Video S6). Interestingly, the coating remains clean without polluting by any dye and oil after repeated soaking in polluted solutions. This phenomenon is understood by the fact that a well-designed micro-/nanostructured surface of the coating can trap a layer of air around them, which protects the surface from being polluted.[53] In total, the reliable thermal and mechanical stability of the superamphiphobic ChNCs-SH-F/SiO_2 coating can satisfy the practical applications of self-cleaning and antifouling.

The ChNCs-SH-F/SiO_2 coating exhibits excellent performance in superamphiphobicity attributed to the synergistic effect of structural characteristics and fluorinated chains. As illustrated in Figure 10, when the coated glass slide is immersed in the water/oil solution, a bright mirrorlike reflection on the surface

https://dx.doi.org/10.1021/acssuschemeng.0c00340
ACS Sustainable Chem. Eng. 2020, 8, 6690−6699

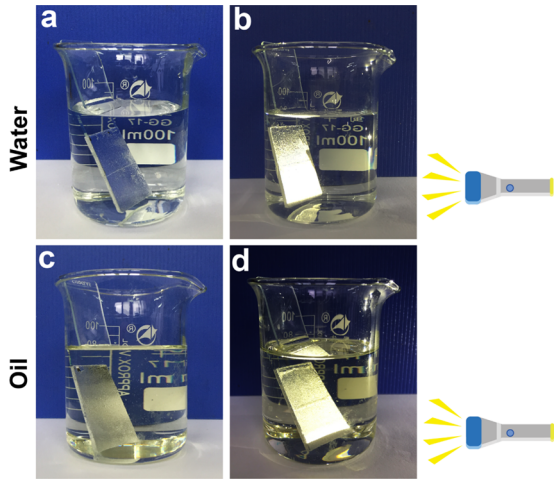

Figure 10. Silver mirrorlike reflection phenomenon of the coated glass slides soaked in water (a, b) (with light) and sunflower seed oil solution (c, d) (with light).

exists at the solid−liquid interface. The surface remains absolutely dry after removing from the solution. Additionally, when the coated glass is placed in the dark, the surface shows a strong light reflection with a flashlight (see Figure 10b,d). There is a layer of air cushion surrounded by the coating, which leads to a total reflection phenomenon. The coating surface is in accordance with the Cassie−Baxter model.[54] That is, once the coating is immersed in the solution, the light enters the air layer (optically thicker medium) from water (optically thinner medium).[55] The light reflection phenomenon of the coating surface confirms that the coating can repel water and organic solvents with superamphiphobicity.

Coatings on Various Substrate Surfaces. To confirm the substrate independence, the superamphiphobic powder is coated on various substrates (nonwoven fabrics, glass, sponge, plastic membrane, cotton, and filter paper). As illustrated in Figure 11, various droplets (water, ethylene glycol, sunflower seed oil, and *n*-hexadecane) can stand on the coated substrates even on different fiber mats and maintain a spherelike shape without liquid-wetting behavior (Figure 11a_1,b_1,c_1,d_1,e_1,f_1). It can be observed in the SEM images that superamphiphobic nanoparticles are randomly bonded on the substrate surfaces, showing a micron-/submicron-sized protrusion structure (Figure 11a_2,b_2,c_2,d_2,e_2,f_2). Apart from the low surface free energy of the fluorinated chains, the protrusion structure of ChNCs-SH-F/SiO_2 particles also contributes to the superamphiphobic property. This demonstrates that the superamphiphobic particles are independent of the substrate types, exhibiting promising potential in self-cleaning coating.

CONCLUSIONS

Superamphiphobic particles based on renewable ChNCs with unique nanostructure grafting of thiol groups and fluorinated groups have been developed for self-cleaning coatings. The prepared fluorinated ChNCs/SiO_2 particles show hierarchical micro-/nanostructures, which can hold up a layer of air cushions at the solid−liquid interface. The particles exhibit high contact angles (>156.2°) and low roll-off angles (<9.3°) toward water and various oils. Water and oil droplets can maintain a spherical shape without adhesion of any powder and loss of liquids upon contacting the ChNCs-SH-F/SiO_2-coated substrates. Water and oil marbles can be formed by dropping the liquids on the particles. The superamphiphobic ChNCs-SH-F/SiO_2 can be coated on different substrates by deposition with double-sided tape, spray-coating, dip-coating, and filtering. The particles coated on various substrate surfaces (nonwoven fabrics, glass, sponge, plastic membrane, cotton, and filter paper) exhibit excellent self-cleaning and antifouling properties. Also, the

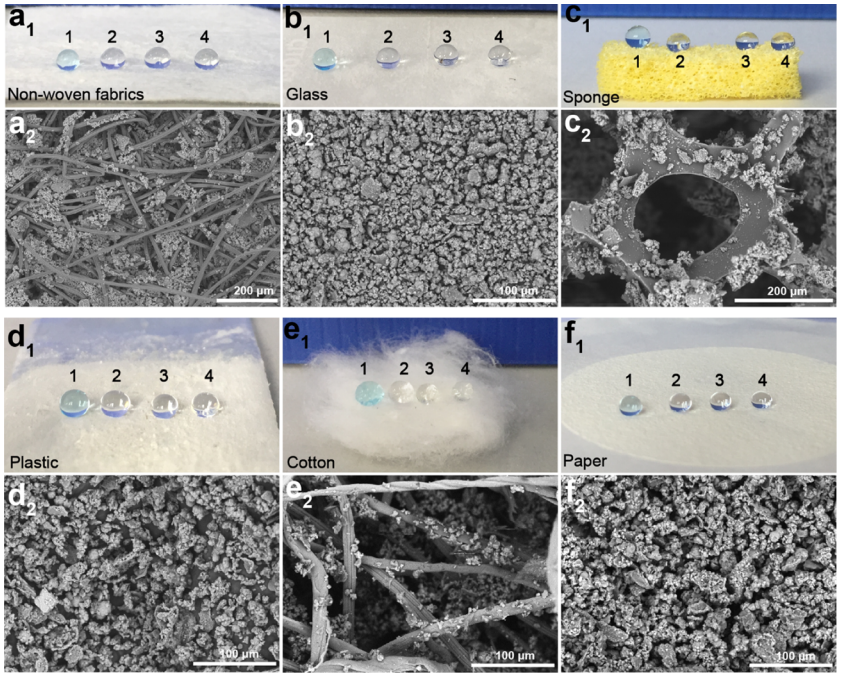

Figure 11. Pictures of different droplets (1: water, 2: ethylene glycol, 3: sunflower seed oil, and 4: *n*-hexadecane) on the coating surfaces and the corresponding SEM images of ChNCs-SH-F/SiO_2-coated nonwoven fabrics (a_1,a_2), glass sheet (b_1,b_2), sponge (c_1,c_2), plastic (d_1,d_2), cotton (e_1,e_2), and filter paper (f_1,f_2).

https://dx.doi.org/10.1021/acssuschemeng.0c00340
ACS Sustainable Chem. Eng. 2020, 8, 6690−6699

mechanical durability and temperature stability can satisfy actual application under harsh conditions. The superamphiphobic fluorinated ChNCs/SiO_2 coatings show great potential in water/oil-proof, self-cleaning, and antifouling applications.

■ ASSOCIATED CONTENT

Supporting Information

The Supporting Information is available free of charge at https://pubs.acs.org/doi/10.1021/acssuschemeng.0c00340.

Interaction test between a water droplet and the coating (Video S1) (AVI)

Interaction test between an oil droplet and the coating (Video S2) (AVI)

Rolling process of liquid marbles on the glass dish (Video S3) (AVI)

Mechanical durability of coated substrates (Video S4) (AVI)

Antifouling test for carbon black dust (Video S5) (AVI)

Antifouling test for dye and oil solution (Video S6) (AVI)

■ AUTHOR INFORMATION

Corresponding Author

Mingxian Liu − *Department of Materials Science and Engineering, Jinan University, Guangzhou 510632, China;* orcid.org/0000-0002-5466-3024; Email: liumx@jnu.edu.cn

Authors

Xianfeng Ou − *Department of Materials Science and Engineering, Jinan University, Guangzhou 510632, China*

Jiabing Cai − *Department of Materials Science and Engineering, Jinan University, Guangzhou 510632, China*

Jinhuan Tian − *Department of Materials Science and Engineering, Jinan University, Guangzhou 510632, China*

Binghong Luo − *Department of Materials Science and Engineering, Jinan University, Guangzhou 510632, China;* orcid.org/0000-0001-8689-4196

Complete contact information is available at: https://pubs.acs.org/10.1021/acssuschemeng.0c00340

Notes

The authors declare no competing financial interest.

■ ACKNOWLEDGMENTS

This work was financially supported by the National Natural Science Foundation of China (51473069 and 51502113), Guangdong Basic and Applied Basic Research Foundation (2019A1515011509), and the Fundamental Research Funds for the Central Universities (21619102).

■ REFERENCES

(1) Liu, M.; Zheng, Y.; Zhai, J.; Jiang, L. Bioinspired super-antiwetting interfaces with special liquid-solid adhesion. *Acc. Chem. Res.* **2010**, *43*, 368−377.

(2) Liu, K.; Yao, X.; Jiang, L. Recent developments in bio-inspired special wettability. *Chem. Soc. Rev.* **2010**, *39*, 3240−3255.

(3) Liu, Y.; Wu, F.; Zhao, X.; Liu, M. High-performance strain sensors based on spirally structured composites with carbon black, chitin nanocrystals, and natural rubber. *ACS Sustainable Chem. Eng.* **2018**, *6*, 10595−10605.

(4) Zorba, V.; Stratakis, E.; Barberoglou, M.; Spanakis, E.; Tzanetakis, P.; Anastasiadis, S. H.; Fotakis, C. Biomimetic artificial surfaces quantitatively reproduce the water repellency of a lotus leaf. *Adv. Mater.* **2008**, *20*, 4049−4054.

(5) Feng, K.; Hong, G.; Liu, J.; Li, M.; Zhou, C.; Liu, M. Fabrication of high performance superhydrophobic coatings by spray-coating of polysiloxane modified halloysite nanotubes. *Chem. Eng. J.* **2018**, *331*, 744−754.

(6) Dong, J.; Zhang, J. Photochromic and super anti-wetting coatings based on natural nanoclays. *J. Mater. Chem. A* **2019**, *7*, 3120−3127.

(7) Yuan, R.; Liu, H.; Chen, Y.; Liu, Z.; Li, Z.; Wang, J.; Jing, G.; Zhu, Y.; Yu, P.; Wang, H. Design ambient-curable superhydrophobic/electroactive coating toward durable pitting corrosion resistance. *Chem. Eng. J.* **2019**, *374*, 840−851.

(8) Wang, L.; Gong, Q.; Zhan, S.; Jiang, L.; Zheng, Y. Robust anti-icing performance of a flexible superhydrophobic surface. *Adv. Mater.* **2016**, *28*, 7729−7735.

(9) Lai, Y.; Tang, Y.; Gong, J.; Gong, D.; Chi, L.; Lin, C.; Chen, Z. Transparent superhydrophobic/superhydrophilic TiO_2-based coatings for self-cleaning and anti-fogging. *J. Mater. Chem.* **2012**, *22*, 7420−7426.

(10) Liu, Y.; Cao, H.; Chen, S.; Wang, D. Ag nanoparticle-loaded hierarchical superamphiphobic surface on an Al substrate with enhanced anticorrosion and antibacterial properties. *J. Phys. Chem. C* **2015**, *119*, 25449−25456.

(11) Arslan, O.; Aytac, Z.; Uyar, T. Superhydrophobic, hybrid, electrospun cellulose acetate nanofibrous mats for oil/water separation by tailored surface modification. *ACS Appl. Mater. Interfaces* **2016**, *8*, 19747−19754.

(12) Xu, Z.; Zhao, Y.; Wang, H.; Wang, X.; Lin, T. A superamphiphobic coating with an ammonia-triggered transition to superhydrophilic and superoleophobic for oil-water separation. *Angew. Chem., Int. Ed.* **2015**, *54*, 4527−4530.

(13) Feng, J.; Tuominen, M. T.; Rothstein, J. P. Hierarchical superhydrophobic surfaces fabricated by dual-scale electron-beam-lithography with well-ordered secondary nanostructures. *Adv. Funct. Mater.* **2011**, *21*, 3715−3722.

(14) Jin, Y.; Wang, P.; Hou, K.; Lin, Y.; Li, L.; Xu, S.; Cheng, J.; Wen, X.; Pi, P. Superhydrophobic porous surface fabricated via phase separation between polyhedral oligomeric silsesquioxane-based block copolymer and polyethylene glycol. *Thin Solid Films* **2018**, *649*, 210−218.

(15) Wang, T.; Cai, J.; Wu, Y.; Hang, T.; Hu, A.; Ling, H.; Li, M. Applicable superamphiphobic Ni/Cu surface with high liquid repellency enabled by the electrochemical-deposited dual-scale structure. *ACS Appl. Mater. Interfaces* **2019**, *11*, 11106−11111.

(16) Ganesh, V. A.; Dinachali, S. S.; Nair, A. S.; Ramakrishna, S. Robust superamphiphobic film from electrospun TiO_2 nanostructures. *ACS Appl. Mater. Interfaces* **2013**, *5*, 1527−1532.

(17) Yuan, R.; Wu, S.; Yu, P.; Wang, B.; Mu, L.; Zhang, X.; Zhu, Y.; Wang, B.; Wang, H.; Zhu, J. Superamphiphobic and electroactive nanocomposite toward self-cleaning, antiwear, and anticorrosion coatings. *ACS Appl. Mater. Interfaces* **2016**, *8*, 12481−12493.

(18) Dong, J.; Wang, Q.; Zhang, Y.; Zhu, Z.; Xu, X.; Zhang, J.; Wang, A. Colorful superamphiphobic coatings with low sliding angles and high durability based on natural nanorods. *ACS Appl. Mater. Interfaces* **2017**, *9*, 1941−1952.

(19) Ma, W.; Higaki, Y.; Takahara, A. Superamphiphobic coatings from combination of a biomimetic catechol-bearing fluoropolymer and halloysite nanotubes. *Adv. Mater. Interfaces* **2017**, *4*, No. 1700907.

(20) Liu, Y.; Liu, M.; Yang, S.; Luo, B.; Zhou, C. Liquid crystalline behaviors of chitin nanocrystals and their reinforcing effect on natural rubber. *ACS Sustainable Chem. Eng.* **2018**, *6*, 325−336.

(21) Ravi Kumar, M. N. V. Chitin and chitosan fibres: a review. *Bull. Mater. Sci.* **1999**, *22*, 905−915.

(22) Zeng, J.; He, Y.; Li, S.; Wang, Y. Chitin whiskers: an overview. *Biomacromolecules* **2012**, *13*, 1−11.

(23) Gopalan Nair, K.; Dufresne, A.; Gandini, A.; Belgacem, M. N. Crab shell chitin whiskers reinforced natural rubber nanocomposites. 3. effect of chemical modification of chitin whiskers. *Biomacromolecules* **2003**, *4*, 1835−1842.

(24) Lu, Y.; Weng, L.; Zhang, L. Morphology and properties of soy protein isolate thermoplastics reinforced with chitin whiskers. *Biomacromolecules* **2004**, *5*, 1046−1051.

(25) Choi, J.; Mun, J.; Wang, M. C.; Ashraf, A.; Kang, S. W.; Nam, S. Hierarchical, dual-scale structures of atomically thin MoS_2 for tunable wetting. *Nano Lett.* **2017**, *17*, 1756−1761.
(26) Lee, W. K.; Jung, W. B.; Nagel, S. R.; Odom, T. W. Stretchable superhydrophobicity from monolithic, three-dimensional hierarchical wrinkles. *Nano Lett.* **2016**, *16*, 3774−3779.
(27) Wang, K.; Liu, X.; Tan, Y.; Zhang, W.; Zhang, S.; Li, J.; Huang, A. Highly fluorinated and hierarchical HNTs/SiO_2 hybrid particles for substrate-independent superamphiphobic coatings. *Chem. Eng. J.* **2019**, *359*, 626−640.
(28) Ma, W.; Wu, H.; Higaki, Y.; Takahara, A. Halloysite nanotubes: green nanomaterial for functional organic-inorganic nanohybrids. *Chem. Rec.* **2018**, *18*, 986−999.
(29) Wu, F.; Pickett, K.; Panchal, A.; Liu, M.; Lvov, Y. Superhydrophobic polyurethane foam coated with polysiloxane-modified clay nanotubes for efficient and recyclable oil absorption. *ACS Appl. Mater. Interfaces* **2019**, *11*, 25445−25456.
(30) Gholami, T.; Salavati-Niasari, M.; Bazarganipour, M.; Noori, E. Synthesis and characterization of spherical silica nanoparticles by modified stöber process assisted by organic ligand. *Superlattices Microstruct.* **2013**, *61*, 33−41.
(31) Zhang, D.; Liu, C.; Chen, S.; Zhang, J.; Cheng, J.; Miao, M. Highly efficient preparation of hyperbranched epoxy resins by UV-initiated thiol-ene click reaction. *Prog. Org. Coat.* **2016**, *101*, 178−185.
(32) Lu, Y.; Sathasivam, S.; Song, J.; Crick, C. R.; Carmalt, C. J.; Parkin, I. P. Robust self-cleaning surfaces that function when exposed to either air or oil. *Science* **2015**, *347*, 1132−1135.
(33) Lin, N.; Zhao, S.; Gan, L.; Chang, P. R.; Xia, T.; Huang, J. Preparation of fungus-derived chitin nanocrystals and their dispersion stability evaluation in aqueous media. *Carbohydr. Polym.* **2017**, *173*, 610−618.
(34) Zhang, H.; Ma, Y.; Tan, J.; Fan, X.; Liu, Y.; Gu, J.; Zhang, B.; Zhang, H.; Zhang, Q. Robust, self-healing, superhydrophobic coatings highlighted by a novel branched thiol-ene fluorinated siloxane nanocomposites. *Compos. Sci. Technol.* **2016**, *137*, 78−86.
(35) Vilcnik, A.; Jerman, I.; Kozelj, M.; Orel, B.; Tomsic, B.; Simoncic, B.; Kovac, J.; Surca Vuk, A. Structural properties and antibacterial effects of hydrophobic and oleophobic sol-gel coatings for cotton fabrics. *Langmuir* **2009**, *25*, 5869−5880.
(36) Zhao, X.; Su, Y.; Liu, Y.; Li, Y.; Jiang, Z. Free-standing graphene oxide-palygorskite nanohybrid membrane for oil/water separation. *ACS Appl. Mater. Interfaces* **2016**, *8*, 8247−8256.
(37) Wang, J.; Wang, Z.; Li, J.; Wang, B.; Liu, J.; Chen, P.; Miao, M.; Gu, Q. Chitin nanocrystals grafted with poly(3-hydroxybutyrate-co-3-hydroxyvalerate) and their effects on thermal behavior of PHBV. *Carbohydr. Polym.* **2012**, *87*, 784−789.
(38) Guo, X.; Xue, C.; Jia, S.; Ma, J. Mechanically durable superamphiphobic surfaces via synergistic hydrophobization and fluorination. *Chem. Eng. J.* **2017**, *320*, 330−341.
(39) Lakshmi, R. V.; Bera, P.; Anandan, C.; Basu, B. J. Effect of the size of silica nanoparticles on wettability and surface chemistry of sol-gel superhydrophobic and oleophobic nanocomposite coatings. *Appl. Surf. Sci.* **2014**, *320*, 780−786.
(40) Li, J.; Yan, L.; Ouyang, Q.; Zha, F.; Jing, Z.; Li, X.; Lei, Z. Facile fabrication of translucent superamphiphobic coating on paper to prevent liquid pollution. *Chem. Eng. J.* **2014**, *246*, 238−243.
(41) Zhu, X.; Zhang, Z.; Xu, X.; Men, X.; Yang, J.; Zhou, X.; Xue, Q. Facile fabrication of a superamphiphobic surface on the copper substrate. *J. Colloid Interface Sci.* **2012**, *367*, 443−449.
(42) Zahid, M.; Heredia-Guerrero, J. A.; Athanassiou, A.; Bayer, I. S. Robust water repellent treatment for woven cotton fabrics with eco-friendly polymers. *Chem. Eng. J.* **2017**, *319*, 321−332.
(43) Wu, X.; Wyman, I.; Zhang, G.; Lin, J.; Liu, Z.; Wang, Y.; Hu, H. Preparation of superamphiphobic polymer-based coatings via spray- and dip-coating strategies. *Prog. Org. Coat.* **2016**, *90*, 463−471.
(44) Rolo, L. I.; Caço, A. I.; Queimada, A. J.; Marrucho, I. M.; Coutinho, J. A. P. Surface tension of heptane, decane, hexadecane, eicosane, and some of their binary mixtures. *J. Chem. Eng. Data* **2002**, *47*, 1442−1445.
(45) Shaker, M.; Salahinejad, E. A combined criterion of surface free energy and roughness to predict the wettability of non-ideal low-energy surfaces. *Prog. Org. Coat.* **2018**, *119*, 123−126.
(46) Rajendra Kumar, R. T.; Mogensen, K. B.; Bøggild, P. Simple approach to superamphiphobic overhanging silicon nanostructures. *J. Phys. Chem. C* **2010**, *114*, 2936−2940.
(47) Gao, N.; Ke, W.; Fan, Y.; Xu, N. Evaluation of the oleophilicity of different alkoxysilane modified ceramic membranes through wetting dynamic measurements. *Appl. Surf. Sci.* **2013**, *283*, 863−870.
(48) Yang, S.; Wang, J.; Ogino, K.; Valiyaveettil, S.; Ober, C. K. Low-surface-energy fluoromethacrylate block copolymers with patternable elements. *Chem. Mater.* **2000**, *12*, 33−40.
(49) Dong, J.; Wang, Q.; Zhang, Y.; Zhu, Z.; Xu, X.; Zhang, J.; Wang, A. Colorful superamphiphobic coatings with low sliding angles and high durability based on natural nanorods. *ACS Appl. Mater. Interfaces* **2017**, *9*, 1941−1952.
(50) Zhang, H.; Liu, Y.; Hou, C.; Ma, Y.; Zhang, B.; Zhang, H.; Zhang, Q. Low-maintenance superamphiphobic coating based on a smart two-layer self-healing network. *Surf. Coat. Technol.* **2017**, *331*, 97−106.
(51) Bian, H.; Dong, X.; Chen, S.; Dong, D.; Zhang, N. Polymer brushes on hydrogen-terminated silicon substrates via stable SiC bond. *Chin. Chem. Lett.* **2018**, *29*, 171−174.
(52) Xiong, L.; Kendrick, L. L.; Heusser, H.; Webb, J. C.; Sparks, B. J.; Goetz, J. T.; Guo, W.; Stafford, C. M.; Blanton, M. D.; Nazarenko, S.; Patton, D. L. Spray-deposition and photopolymerization of organic-inorganic thiol-ene resins for fabrication of superamphiphobic surfaces. *ACS Appl. Mater. Interfaces* **2014**, *6*, 10763−10774.
(53) Chen, L.; Guo, Z.; Liu, W. Biomimetic multi-functional superamphiphobic FOTS-TiO_2 particles beyond lotus leaf. *ACS Appl. Mater. Interfaces* **2016**, *8*, 27188−27198.
(54) Qing, Y.; Long, C.; An, K.; Hu, C.; Liu, C. Sandpaper as template for a robust superhydrophobic surface with self-cleaning and anti-snow/icing performances. *J. Colloid Interface Sci.* **2019**, *548*, 224−232.
(55) Li, Y.; Li, B.; Zhao, X.; Tian, N.; Zhang, J. Totally waterborne, nonfluorinated, mechanically robust, and self-healing superhydrophobic coatings for actual anti-icing. *ACS Appl. Mater. Interfaces* **2018**, *10*, 39391−39399.

https://dx.doi.org/10.1021/acssuschemeng.0c00340
ACS Sustainable Chem. Eng. 2020, 8, 6690−6699